3.4 Simplified Theoretical Methods for Aerodynamic Design

Jan R. Tulinius
NASA Langley Research Center

Introduction

The objective of this paper is to describe theoretical procedures which can be utilized by the general aviation industry for aerodynamic design. It is recognized that the general aviation industry has a requirement for a wide range of levels of sophistication in aerodynamic design. However, very simple procedures requiring minimum computer size and operational costs, coupled with minimum input effort and maximum numerical stability, are in general required.

This paper is organized to first discuss the design process and theoretical methods used to design a wing. Then theoretical methods for estimating the interference velocities due to the fuselage, or other bodies, and nacelles are discussed. It is assumed that the flow fields due to the different components can be superimposed, and then the pressure coefficients computed from the Bernoulli equation.

Methods to estimate the induced, viscous form, and compressible drags are also discussed.

In addition, a procedure for modifying the surface contours to reduce adverse pressure distributions induced by component interference is discussed.

Source/Vortex Lattice

In order to theoretically design a finite aspect ratio wing, it is necessary to have a thick-lifting-surface theory. If the boundary conditions are linearized, the flow fields induced by the wing can be divided into two parts: (1) the flow field due to lift; and (2) the flow field due to thickness. Also, due to the linearization, the perturbation velocity due to lift can be linearly related to the local angle of attack of the mean camber surface and the perturbation velocity due to thickness can be linearly related to the freestream component of the gradient of the thickness distribution.

The most simplified thick-lifting-surface theory is the source/vortex lattice shown in Figure 1. The vortex lattice is a system of lifting lines where one lifting line is placed on each quadrilateral panel of the wing. The source lattice is analogous to the lifting line, except that the velocities induced by a source line

are rotated 90° to that induced by a vortex line. Also, the vortex lines cannot end in space, and, therefore, there must be trailing legs going off to infinity. The vortex lines are usually placed at the quarter chord of each panel and the source lines at both the quarter and three-quarter chord points of each panel. The wing surface velocities are computed at the three-quarter-chord point. Derivations of the influence equations for the source/vortex lattice along with second order corrections for blunt leading edges, interference between thickness and lift, and compressibility are given in References 1 and 2.

The source/vortex lattice can be used to solve for the surface pressures for a given wing twist, camber, angle of attack, and thickness distribution, or it can be used to solve for the wing twist, camber, angle of attack, and thickness distribution for a desired set of surface pressures.

Figure 2 describes how the wing can be designed using the source/vortex lattice. If an airfoil has been designed with the desired section properties, the wing surface shape, which will produce the same upper and lower surface pressures as the two-dimensional airfoil, can be solved for using the approach shown on the left side of Figure 2.

If no two-dimensional design is available, with the desired section characteristics, the second approach shown on the right side of Figure 2 can be used. This approach is analogous to the two-dimensional "ideal angle of attack" design technique discussed in Reference 3. Essentially what this design procedure does is define a wing which has minimum induced drag at the design lift coefficient and a minimum adverse leading-edge pressure gradient, for low viscous form drag, at what is defined as $C_{L_{OPT.}}$ in Figure 2.

As shown in Figure 2, this design procedure gives the wing camber and twist such that the induced-drag polar is tangent to the locus of minimum induced drags at C_{L_D} and the zero percent suction polar is tangent to the induced-drag polar at $C_{L_{OPT.}}$. The data should fall somewhere between these two polars. The zero percent suction drag is defined as that for which there is no thrust at the leading edge of the section.

General Slender Body Theory

General slender body theory can be used to compute the flow fields due to arbitrary shaped fuselages or other bodies. The theory requires access to only a body of revolution and a two-dimensional airfoil theory. The arbitrary body flow fields are computed, as depicted in Figure 3, by superimposing the flow fields from

the equivalent body of revolution plus a correction for the noncircular cross-section, which is computed with a two-dimensional airfoil program.

The correction flow field due to the noncircular cross-section is obtained by subtracting the two-dimensional solution for the circular cross-section from that for the noncircular cross-section. These solutions are obtained using the full three-dimensional boundary conditions in the two-dimensional airfoil program. The difference between the usual two-dimensional boundary conditions, which would represent the effects due to angle of attack and sideslip, and the three-dimensional boundary conditions is the effect due to body growth in the longitudinal direction.

There are several possible variations to the solution of the general slender body problem. Langley Research Center is in the process of developing a version which will be coupled with a thick-lifting-surface theory. A derivation of the theory is given in Reference 4.

The application of this theory and its component parts are listed in Figure 4.

Induced-Drag Analysis and Design

The induced drag of an arbitrary lifting system can be computed by an equivalent lifting line in the Trefftz plane. Figure 5 depicts the equivalent lifting line as seen from an end view. The dots represent the trailing legs of the horse-shoe vortices pointing out of the paper. The bound vortex line segments between the dots have circulation strengths equal to Γ. The line can be bent to represent any arbitrary wake shape. Also, any number of wakes can be represented to account for multiple lifting surfaces such as horizontal tails, canards, fins, and vertical tails as well as the wing. End plates or winglets can also be represented by this method.

As listed in Figure 6, the theory can be used to solve for not only the drag of a given configuration, after the span loads have been computed by the source/vortex lattice theory, but due to the quadratic nature of the drag expression, the optimum span loads can also be computed for both trimmed and untrimmed conditions using the method of Lagrange multipliers.

A computer program has been developed at Langley Research Center by Blair Gloss and the author to compute the induced drag for given span loads or solve for optimum span loads utilizing the equation in Figure 5. This equation is derived in Reference 1.

Viscous Form Drag

The viscous form drag is due to the boundary layer giving the airfoil section an effective change in shape due to the displacement thickness. As listed in Figure 7, the viscous form drag can be estimated from two-dimensional experimental drag polars at each span station along the wing, utilizing the wing section lift coefficient, and then integrating. This approach is presently being developed by Professor Ralph Krenkel of the Polytechnic Institute of New York under a NASA grant from Langley Research Center.

The viscous form drag can also be computed using an infinite yawed wing boundary-layer program at a series of span stations and then integrating. This approach is being presently worked on at Langley utilizing a boundary-layer program developed by Frank Dvorak and Frank Woodward (Ref. 5). In this approach, equivalent airfoils are developed at each span station which produce the same pressure distributions in two-dimensional flow as is developed by the actual section on the finite wing in three-dimensional flow. These airfoils are then run through the infinite yawed wing boundary-layer program to determine the section viscous form drag.

A third procedure, which is most appropriate during preliminary design, is to utilize a percent suction versus C_L curve from a configuration with similar section properties. This curve, shown in Figure 8, is obtained by the following equation:

$$\% \text{ suction} = \frac{C_L^{2/}C_{L_\alpha} - \left(C_D - C_{D_o}\right)}{C_L^{2/}C_{L_\alpha} - C_L^{2/}\pi AR} \times 100$$

The two boundary curves defined by $C_L^{2/}C_{L_\alpha}$ and $C_L^{2/}\pi AR$ are the upper and lower bounds, respectively. The location of the data relative to these two curves is primarily a function of viscous effects due to the section shape. As can be seen in Figure 8, the GA(W)-1 section has good characteristics up to a $C_L = 1.2$. The theory shown on this figure is from a vortex-lattice program developed by the author.

Compressible Drag

The compressible drag for conventional airfoils can be estimated using the crest theory. The crest theory states that drag divergence will occur shortly after the crest of the airfoil becomes sonic. The crest is defined as that point on the airfoil where the free stream is tangent to the airfoil surface. The critical pressure

coefficient is defined on Figure 9. It should be noted that it is a function of both sweep and the free-stream Mach number.

Once the Mach number for drag divergence M_{DD} is known, then an incremental drag due to compressibility can be obtained from an empirical curve of ΔC_{D_C} versus M/M_{DD}. This increment is then added to the incompressible drag obtained from the sum of the skin friction drag, induced drag, and viscous form drag.

Contour Modifications due to Interference Effects

With the procedures discussed in the previous sections, the surface pressures and associated pressure drag and lift can be estimated for a complete aircraft. Since the wing alone was designed to have an optimum pressure distribution, the addition of the fuselage, tip tanks, and nacelles will deteriorate the wing-alone design. These interference effects can be minimized by modifying the component contours to relieve the unfavorable interference pressures.

The incremental pressures due to the interference can be converted to incremental velocities through the use of the Bernoulli equation. As much of this increment as possible should be relieved by judicious placement of the components. Then the remainder should be minimized by locally contouring adjacent components.

The change in wing shape to account for flow induced by another component can be solved for by means of the relationship between velocity and the slope of the surface given in Figure 1. If the induced velocity is primarily in the chord direction, the thickness can be modified by the process outlined in Figure 10.

The contour modification might have to be divided between the wing thickness and the adjacent component surface. If the adjacent component is a body, approximately twice as big a slope change must be made for the same change in velocity as is needed on the wing. This is due to the fact that the perturbation velocity produced by a two-dimensional contour is about twice as large as that produced by a body. This is only an approximate rule of thumb. However, for the case of a sphere and a cylinder, the difference is exactly twice.

If the induced flow is perpendicular to the chord, then a twist and camber modification will be needed. In this case, it is just necessary to change the mean camber surface angle of attack by an amount equal to the induced angle of attack.

Conclusions

There exist sufficient simplified theories applicable to the design of general aviation aircraft. However, most of these theories have not been programmed for general aviation design purposes, and in many cases, the computer programs and their application have not been published in the open literature.

Langley Research Center is supporting the development of programs, utilizing these theories, which will be sized for general aviation purposes. Some of these programs are being developed by center researchers and others under university grants. A significant portion of this capability will be available a year from now.

References

1. Tulinius, J., Clever, W., Niemann, A., Dunn, K., and Gaither, B., "Theoretical Prediction of Airplane Stability Derivatives at Subcritical Speeds," NASA CR-132681, 1975.
2. Tulinius, J., "Theoretical Prediction of Thick Wing and Pylon-Fuselage-Fanpod-Nacelle Aerodynamic Characteristics at Subcritical Speeds," NASA CR-137578, 1974.
3. Abbott, I., and von Doenhoff, A., Theory of Wing Sections, Dover Publications, Inc., 1959.
4. Ashley, H., and Landahl, M., Aerodynamics of Wings and Bodies, Addison-Wesley Publishing Co., Inc., 1965.
5. Dvorak, F., and Woodward, F., "A Viscous/Potential Flow Interaction Analysis Method for Multi-Element Infinite Swept Wings," NASA CR-2476, 1974.

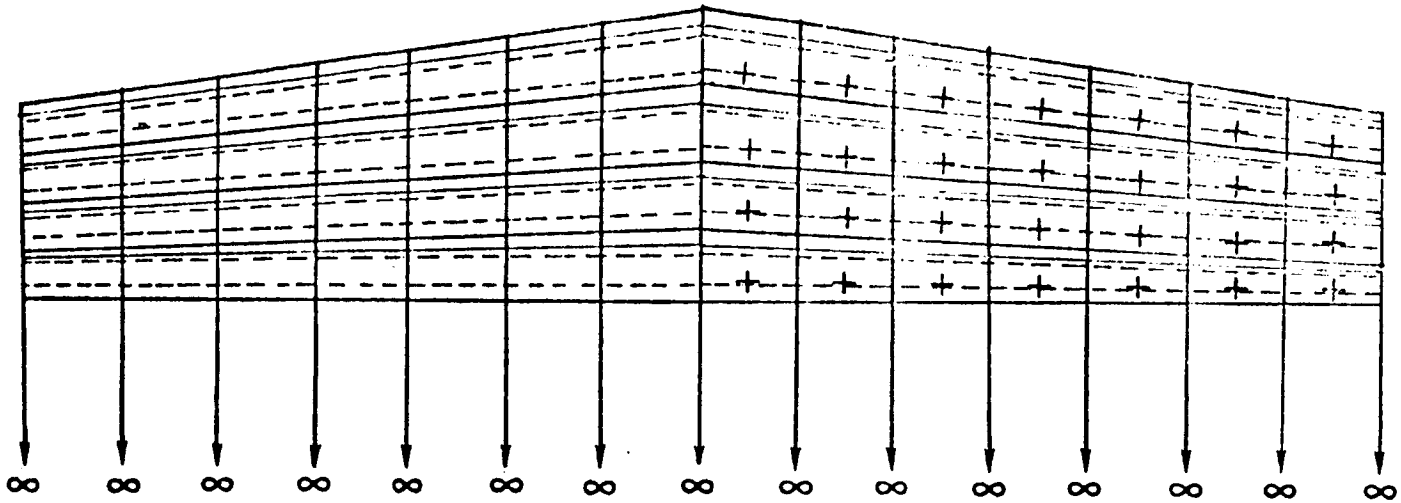

PANEL EDGES

SOURCE LINES

VORTEX LINES

\+ CONTROL POINTS

$$\left\{\frac{V_t}{V_\infty}\right\} = \left[S\right]\left\{\frac{dz_t}{dx}\right\}$$

$$\left\{\alpha\right\} = \left[A\right]\left\{\frac{V_\ell}{V_\infty}\right\}$$

Figure 1. Source/Vortex Lattice Analysis and Design Method

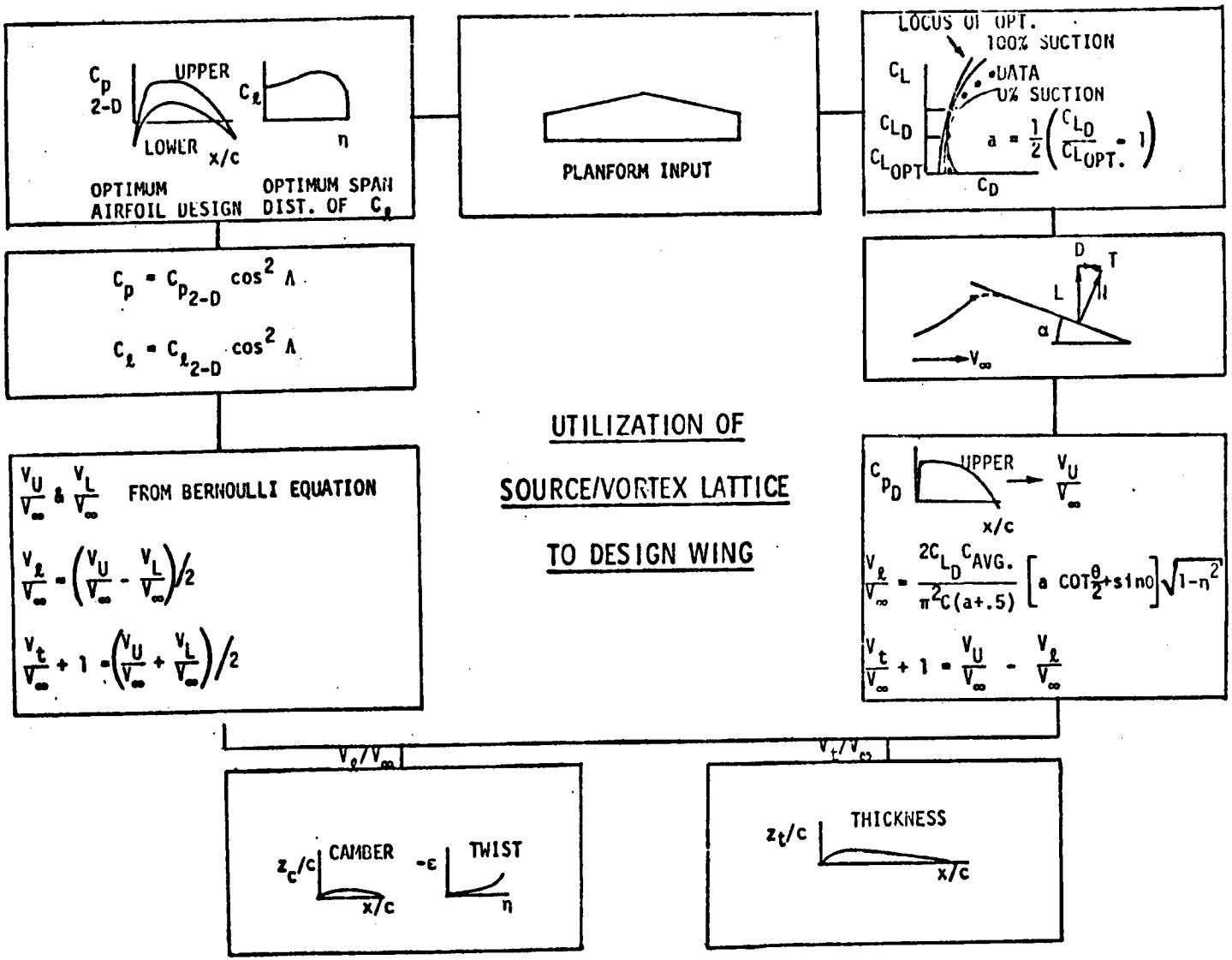

Figure 2. Utilization of Source/Vortex Lattice to Design Wing

FLOW FIELD AT ANY POINT DUE TO AN ARBITRARY BODY IS GIVEN BY SUPERPOSITION:

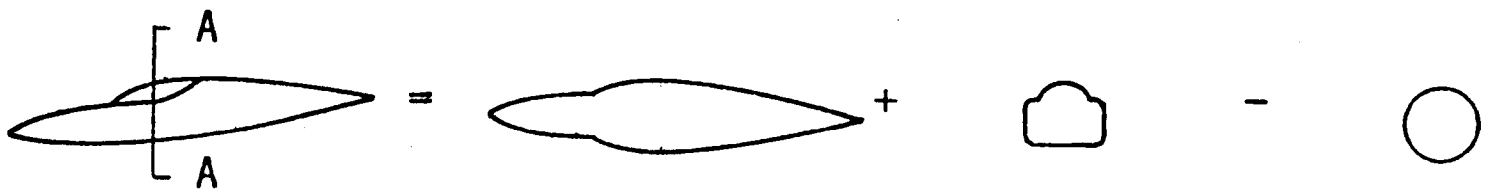

FLOW FIELD DUE TO ACTUAL BODY = SOLUTION FOR EQUIVALENT BODY OF REVOLUTION + 2-D SOLUTION FOR ACTUAL BODY CROSS-SECTION A-A - 2-D SOLUTION FOR EQUIVALENT CROSS-SECTION A-A

3-D BOUNDARY CONDITIONS ARE SATISFIED IN THESE 2-D SOLUTIONS

Figure 3. General Slender Body Theory

MAIN CAPABILITY

- COMBINE GENERAL SLENDER BODY THEORY WITH SOURCE/VORTEX LATTICE TO OBTAIN:
  - Velocities tangent to wing surface due to the fuselage and other bodies
  - Upwash on the wing due to the fuselage and other bodies

ADDITIONAL CAPABILITY

- USE BODY OF REVOLUTION PORTION OF SOLUTION TO OBTAIN VELOCITIES INDUCED BY NACELLES
- USE 2-D PORTION OF SOLUTION TO EVALUATE AIRFOIL DESIGNS

Figure 4. Utilization of General Slender Body Theory

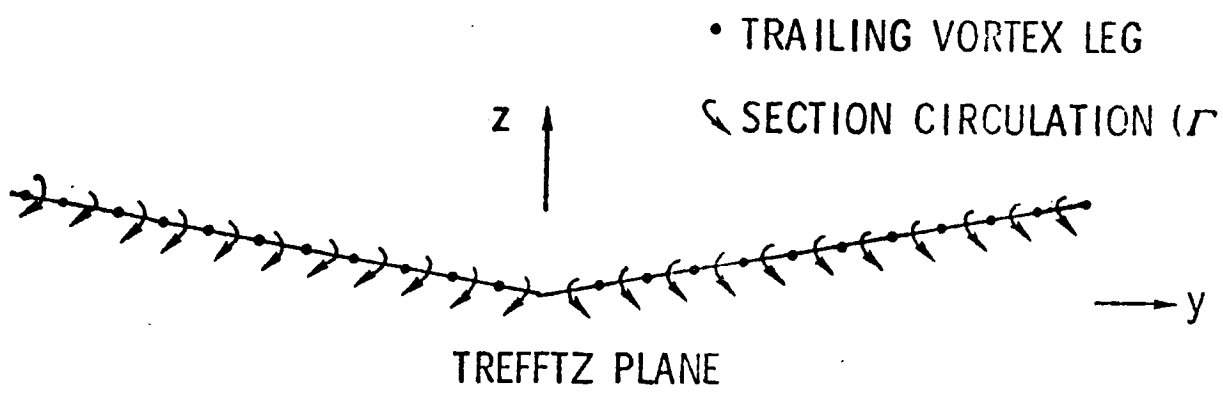

$$C_{D_i} = \frac{AR}{2\pi b^2} \sum_{j=1}^{n} \sum_{k=1}^{n} \left(\frac{\Gamma}{V_\infty}\right)_j \left(\frac{\Gamma}{V_\infty}\right)_k \left[\left(E_{v_{jk}} T_{y_k} + E_{w_{jk}} N_{y_k}\right) T_{z_j} - \left(E_{v_{jk}} T_{z_k} + E_{w_{jk}} N_{z_k}\right) T_{y_j}\right] \Delta S_j$$

$\vec{T}$ UNIT VECTOR TANGENT TO WAKE

$\vec{N}$ UNIT VECTOR NORMAL TO WAKE

ΔS_j INCREMENTAL SECTION WIDTH

E_v y COMPONENT OF INFLUENCE FUNCTION FOR PAIR OF TRAILING LEGS

E_w z COMPONENT OF INFLUENCE FUNCTION FOR PAIR OF TRAILING LEGS

Figure 5. Induced Drag Analysis and Design Method

- COMPUTE INDUCED DRAG
  - WING WITH ARBITRARY DISTRIBUTION OF DIHEDRAL
  - MULTIPLE LIFTING SURFACES
- COMPUTE OPTIMUM SPAN LOADS FOR TRIMMED CONDITIONS

Figure 6. Utilization of Induced Drag Trefftz Plane Method

- AIRFOIL DRAG POLAR DATA APPLIED ALONG STRIPS

- BOUNDARY-LAYER STRIP ANALYSIS
  - SOLVE FOR EQUIVALENT AIRFOIL TO SUPPORT 3-D POTENTIAL PRESSURE DISTRIBUTIONS
  - UTILIZE INFINITE YAWED BOUNDARY-LAYER PROCEDURE

- EMPIRICAL PERCENT SUCTION METHOD
  - UTILIZE PERCENT SUCTION VERSUS C_L CURVE FROM CONFIGURATION WITH SIMILAR SECTION CHARACTERISTICS

Figure 7. Viscous Form Drag Analysis

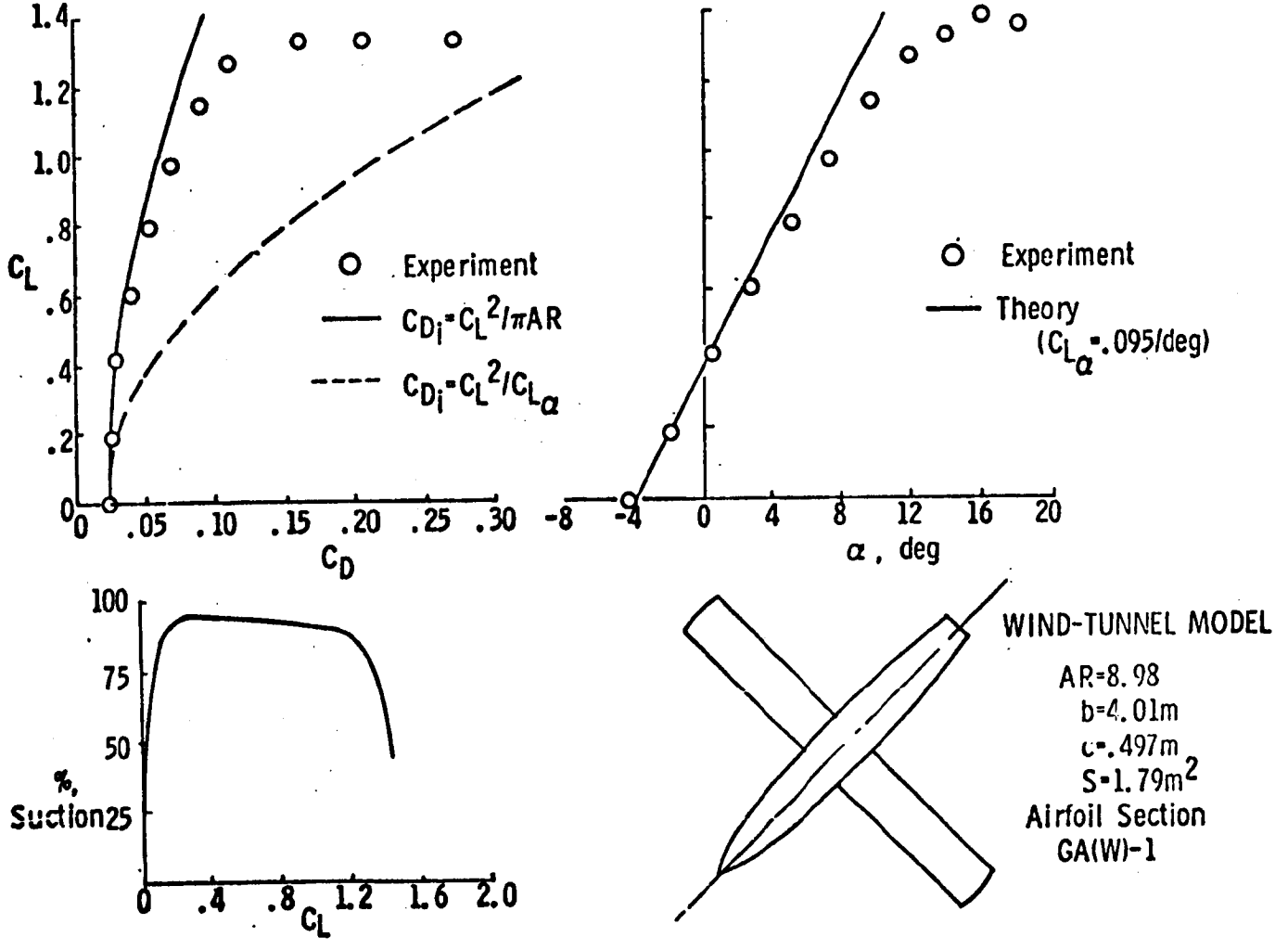

Figure 8. Aerodynamic Characteristics of General Aviation Model

- CALCULATE C_L AND MACH NUMBER AT WHICH THE PRESSURE COEFFICIENT AT THE CREST OF THE AIRFOIL BECOMES CRITICAL

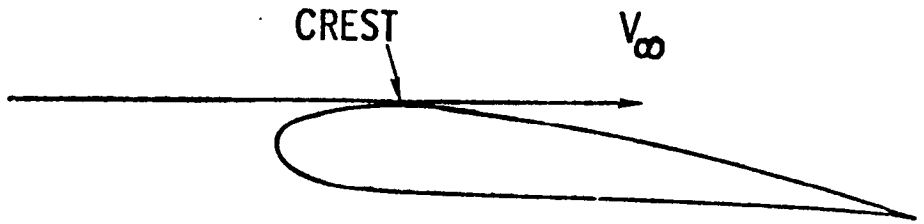

$$C_p^* = \frac{2}{\gamma M_\infty^2}\left[\left\{\frac{2}{\gamma+1}\left(1+\frac{\gamma-1}{2}M_\infty^2\cos^2\Lambda\right)\right\}^{\gamma/(\gamma-1)} - 1\right]$$

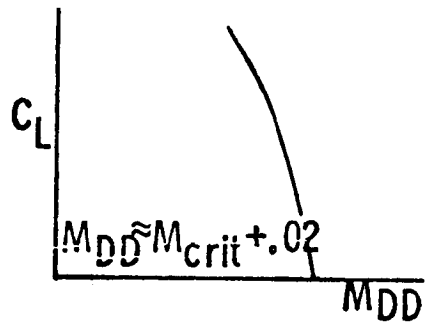

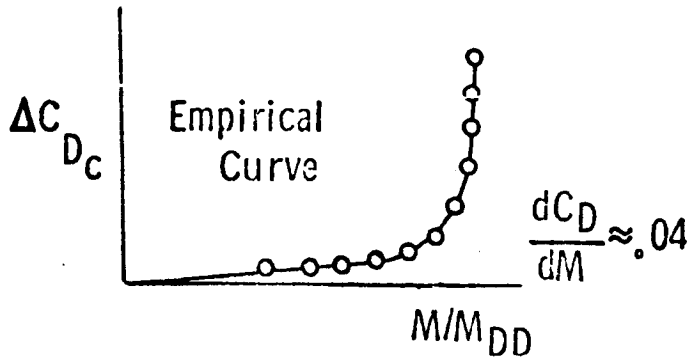

Figure 9. Compressible Drag

- UNFAVORABLE INDUCED WING SURFACE VELOCITIES
  - SOLVE FOR Δz_t UTILIZING

$$\left\{\frac{\Delta V_t}{V_\infty}\right\} = \left[S\right] \left\{\Delta \frac{dz_t}{dx}\right\}$$

  - APPLY NEGATIVE Δz_t TO WING CONTOUR
  - APPLY NEGATIVE $\approx 2\,\Delta z_t$ TO ADJACENT BODY CONTOUR

Figure 10. Contour Modification to Relieve Unfavorable Interference Effects